JOURNAL OF GEOPHYSICAL RESEARCH, VOL. 106, NO. D9, PAGES 9673–9683, MAY 16, 2001

Distribution of vegetation in wind-dominated landscapes: Implications for wind erosion modeling and landscape processes

Gregory Stewart Okin

Department of Geography, University of California, Santa Barbara, California

Dale A. Gillette

Atmospheric Sciences Modeling Division, Air Resources Laboratory, National Oceanic and Atmospheric Administration, Research Triangle Park, North Carolina

Abstract. Dust emission and wind erosion from arid and semiarid environments provide a major source of global atmospheric aerosols. Well-known relations between wind stress and saltation sand flux for sand sheets and relations between sand flux and dust emission by sandblasting have enabled construction of dust models that have only been partly successful in predicting atmospheric mineral dust concentrations. Most models of wind erosion assume that vegetation is evenly distributed. Through the use of field, Fourier transform, and semivariogram analysis, we show that mesquite dunelands in the Chihuahuan Desert of southern New Mexico, United States, have anisotropic shrub distributions. Elongated areas of bare soil, "streets," which are aligned with the prevailing winds may partially explain discrepancies between observed and predicted atmospheric dust concentrations. Soils in the streets are not protected from winds blowing down the streets and may therefore produce more dust than if vegetation were more evenly distributed. Currently, few desert landscape evolution models take the role of wind explicitly into account. The existence of streets implies that wind plays a major role in the evolution of vegetated arid and semiarid landscapes with wind-erodible soils. Here wind acts in tandem with water to enforce islands of fertility centered around individual shrubs and may provide an explanation for reduced soil fertility observed in shrublands. Furthermore, in order for mathematical models of dust flux to be successful in these landscapes, new landscape models are required which incorporate the existence and orientation of streets.

1. Introduction

Dust emission and wind erosion from arid and semiarid environments provide a major source of global atmospheric aerosols. Aerosols from deserts and other sources have been suggested as a mechanism for increasing planetary albedo, thus counteracting global warming [*Andreae*, 1996]. Understanding the environmental factors that enhance wind erosion in deserts, therefore, is important in modeling global climate change in the coming century.

At the same time, wind plays an important role in the evolution of arid and semiarid landscapes. While this is most obvious in sand seas and sand dunes common in deserts, wind erosion is also a major component of landscape degradation [*Wilshire*, 1980; *Luk*, 1983; *Çevik and Berkman*, 1985; *El-Baz et al.*, 1985; *Kishk*, 1985; *Zhao*, 1985; *Darkoh*, 1987; *Khalaf*, 1989; *Leys and McTainsh*, 1996; *Ayoub*, 1998; *Bach*, 1998; *Barth*, 1999]. Wind erosion tends to enforce the concentration of soil resources in islands of fertility [*Schlesinger et al.*, 1990]. It is thus important to understand the detailed mechanisms by which wind interacts with the land surface.

By combining relations between wind stress and saltation sand flux with relations between sand flux and dust emission by sandblasting, wind erosion models have been constructed which have been partly successful in predicting atmospheric mineral dust concentrations [*Gillette and Passi*, 1988; *Marticorena et al.*, 1997; *Shao and Leslie*, 1997]. However, the effects of vegetation are not directly included in these models. The effects of vegetation have been successfully modeled by approximating the form and spatial distribution of shrubs as regularly distributed solid hemispherical roughness elements on the soil [*Musick and Gillette*, 1990; *Stockton and Gillette*, 1990]. The effect of randomly placed small vegetation patches has been modeled by considering vegetation primarily to cause a change in aerodynamic roughness length [*Marticorena and Bergametti*, 1995]. However, for some vegetation, random placement is not observed, and these models do not apply. For example, *Phinn et al.* [1996] have demonstrated systematic spatial patterns in Chihuahuan Desert mesquite dunelands. For improved models of dust emission, we must understand the role of vegetation in mediating the interaction between the wind and the soil.

Recent research shows that desert areas dominated by mesquite (*Prosopis glandulosa*) plants, which have the same total vegetation biomass as other desert shrublands produce more dust by ratios ranging from 4:1 to 8:1 [*Gillette and Monger*, 2000]. Ground-based observations and investigations of aerial photographs led one of us (DAG) to suggest that mesquite-dominated areas possess significantly elongated areas of bare soil (Figure 1). Further observations pointed to a possibility that these elongated areas of bare soil were preferentially

Paper number 2001JD900052.
0148-0227/01/2001JD900052$09.00

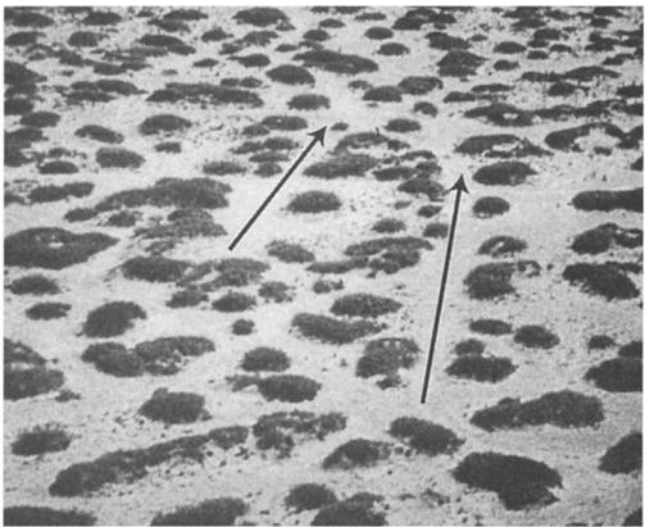

Figure 1. Low-altitude oblique aerial photograph taken of Fort Bliss, New Mexico (Courtesy of H. C. Monger, New Mexico State University). For scale, mesquite bushes at this site are ~2 m in diameter. At this site, which is ~100 km from the Jornada Long-Term Ecological Research site, mesquite bushes are the principal vegetation in coppice dunelands. Notice the elongated "streets" marked through the middle of the photograph.

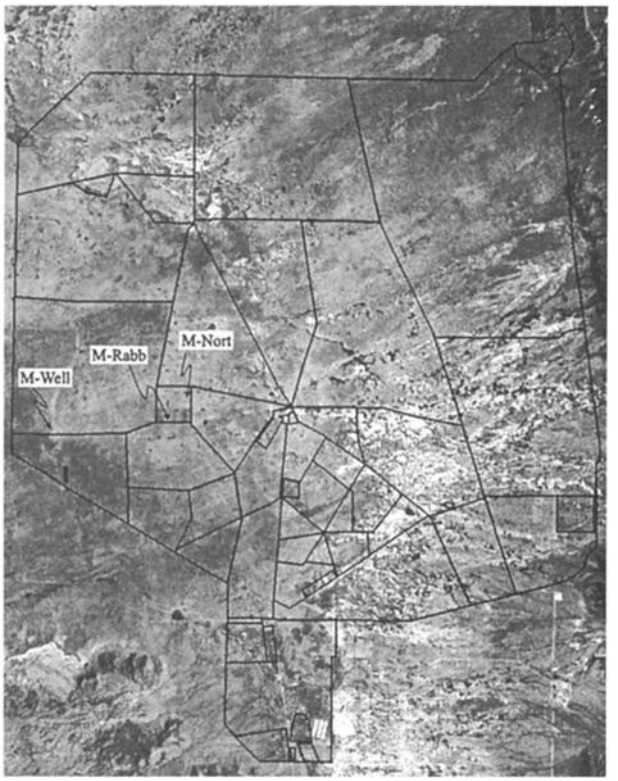

Figure 2. Panchromatic Landsat TM image of the Jornada basin taken July 6, 1992. Pastures within the Jornada LTER site are shown in black. The locations of the three sites used in this study (M-Nort, M-Rabb, M-Well) are shown. These sites are LTER mesquite monitoring sites and are dominated by mesquite coppice dunes.

oriented. Here we define a "street" in an anisotropic landscape with patchy vegetation as a patch of bare soil, the width of which is much less than the length. Many streets may exist in a landscape, and streets can exhibit one or more preferred orientations. If such streets exist and are preferentially oriented in the direction of the strongest winds and most persistent wind direction, they may explain the high mass flux rates observed at mesquite sites compared to sites dominated by other kinds of vegetation. Isotropic landscapes without streets would be expected to have lower relative dust flux rates because average intershrub distances would be smaller, implying that average fetch is less in these landscapes.

The existence of streets in mesquite shrublands is a potentially important diagnostic feature for elevated dust production. The purpose of this study is threefold: (1) using both field mapping and high spatial resolution aerial photographs, we confirm the existence of streets in mesquite dunelands; (2) we develop two image-processing techniques that are able to identify the presence and orientation of streets and can be used generally to identify landscapes with streets; and (3) we address the implications of streets for the evolution of arid and semiarid environments.

2. Experimental Methods

2.1. Experimental Sites

This study was conducted at the Jornada Long-Term Ecological Research (LTER) site 40 km northeast of Las Cruces, New Mexico, in the Chihuahuan Desert ecosystem (Figure 2). It is located on the Jornada del Muerto plain, which is bounded by the San Andres Mountains on the east and by the Rio Grande valley and the Fra Cristobal-Caballo Mountain complex on the west. Elevation varies from 1180 to 1360 m. The Jornada plain consists of unconsolidated Pleistocene detritus. This alluvial fill from the nearby mountains is 100 m thick in places, and the aggradation process is still active. Coarser materials are found near foothills along the eastern part of the study area. The topography of the Jornada basin consists of gently rolling to nearly level uplands, interspersed with swales and old lake beds [*Buffington and Herbel*, 1965].

The climate of the area is characterized by cold winters and hot summers and displays a bimodal precipitation distribution. Winter precipitation usually occurs as low-intensity rains or occasionally as snow and contributes to the greening of shrub species in the basin in the early spring. Summer monsoonal precipitation, usually in the form of patchy but intense afternoon thunderstorms, is responsible for the late-summer greening of grasses. The average annual precipitation between 1915 and 1962 in the basin was 23.1 cm, with 52% falling between July 1 and September 30 [*Paulsen and Ares*, 1962]. The average maximum temperature is highest in June, when it averages 36°C, and lowest in January, when it averages 13°C [*Buffington and Herbel*, 1965].

The principal grass species in the study area are burrograss (*Scleropogon brevifolius*), several species of *Aristida*, and tobosa grass (*Hilaria mutica*), while major shrubs are creosote (*Larrea tridentata*), mesquite (*Prosopis glandulosa*), and tarbush (*Florensia cernua*). Soils in the basin are quite complex but generally range from clay loams to loamy fine sands, with some areas being sandy or gravelly [*Bulloch and Neher*, 1977].

The Jornada LTER site has 15 permanent vegetation monitoring sites, which represent the five dominant vegetation types in the basin: mesquite, creosote, tarbush, playa grasses, and nonplaya grasses. The three net primary production (NPP)

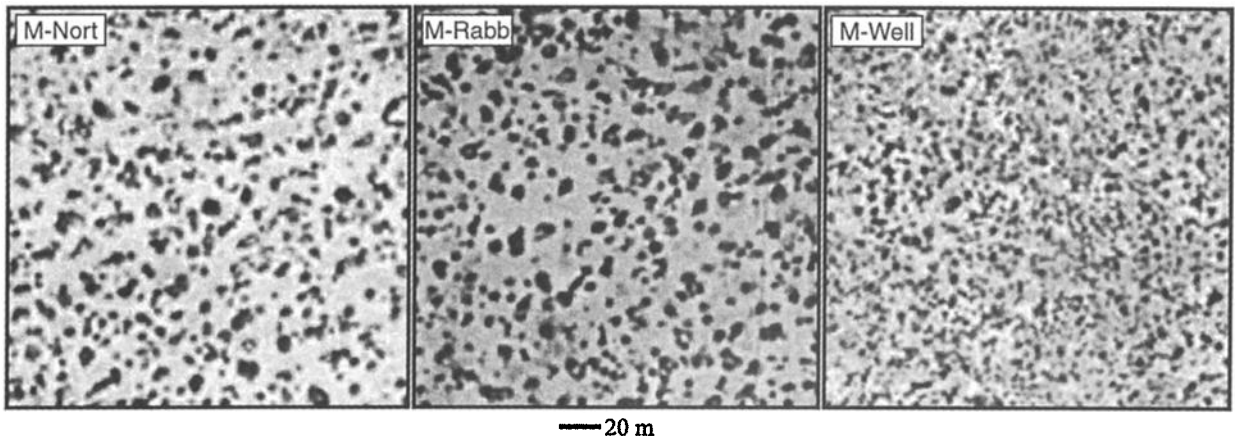

Figure 3. Images of the three mesquite dunelands sites used in this study. Images have 1 m resolution and are taken from the red band of United States Geological Survey digital color orthophoto quadrangles. Each image is 200 by 200 m and north is up. M-Nort and M-Rabb display large shrubs with large intershrub spacing, while M-Well has smaller shrubs closer together.

monitoring sites dominated by mesquite plants (M-Nort, M-Rabb, and M-Well) were used for this study (Figure 2). Also present at these sites is burrograss and yucca. Soils at these sites belong to the very similar Onite-Pajarito and Onite-Pintura associations, which are principally composed of sandy loam overlain by loamy sand [*Bulloch and Neher*, 1977]. All three sites are located on flat plains and are characterized by mesquite coppice dunes. Coppice dune formation is most pronounced at the M-Nort and M-Rabb sites with dunes often greater than 1 m in height. At M-Well site, coppice dunes are less developed and rarely exceed heights of 1 m.

2.2. Mapping and Description of Street Length Versus Wind Direction

Detailed vegetation maps were constructed at M-Nort, M-Rabb, and M-Well during the summer of 1999. Each of these sites possesses different vegetation coverage densities. Field mapping used a square grid with points every 0.5 m. The grids used at M-Nort and M-Well were 50 m by 50 m and that used at M-Rabb was 50 m by 45 m. Mapping areas where chosen to be adjacent to permanent LTER NPP monitoring sites. A cover map was produced which identified three plant categories found at each point of the grid: mesquite, perennials, and yucca. These three categories (predominantly mesquite) covered all the plant types at the two sites. A fourth category was bare soil. The field maps were digitized and condensed into two categories: plant and bare soil.

The digitized maps were used to generate probability distributions for the length of bare soil area versus wind direction. For every grid point on the map, the length of bare soil grid spaces was measured at 12° intervals. This street length versus direction for each point on the grid allowed us to calculate a probability distribution of street length versus direction.

Probability distributions of street length versus direction for the three sites were used to compute expected street length (integral of street length times probability of street length for all street lengths) versus wind direction for the three mesquite sites. The expected street length versus direction for the three sites was used to create plots for each site wherein the expected street length was extended from a central hub along its direction. By using 32 different directions at 12° intervals, a two-dimensional bare soil "rose" was drawn similar to a wind rose diagram (e.g., Figure 5).

2.3. Image Acquisition and Processing

2.3.1. Digital orthophoto quads. Digital orthophoto quads (DOQs) were obtained from the U.S. Geological Survey and were chosen to include the three mesquite NPP sites. DOQs have a ground resolution of 1.0 m and were produced by digitizing USGS color orthophoto quads. The aerial photographs, which are the source data for these images, were acquired in October 1996. The 200 by 200 m subimages containing the mesquite NPP-monitoring sites were extracted from original images, and the red spectral band was used for all subsequent processing (Figure 3).

Digital number (DN) values in these images range from zero to 255 and enable discrimination between green vegetation (low DN values at red wavelengths) and bare soil (high DN values at red wavelengths). Since mesquite shrubs are generally larger than 1 m in diameter and are spaced more than 1 m apart, the resolution of the DOQs is smaller than the scale of spatial variability on the ground. This allowed us to see individual shrubs in the images and to apply two spatial analysis techniques to explore the distribution of individual mesquite shrubs at each of our test sites.

2.3.2. Fourier transform analysis. Two-dimensional Fourier transforms (FT) were performed on each of the mesquite-site subimages (Figure 3) using the fast-FT procedure in the Interactive Data Language (IDL, version 5.3 for Unix). A log-power image was produced by calculating for each cell in the two-dimensional FT images:

$$\log - \text{power} = \log_{10}\sqrt{(\text{real})^2 + (\text{imaginary})^2}, \qquad (1)$$

where real is the real portion of the FT spectrum for each cell and imaginary is the imaginary portion of the FT spectrum for each cell.

The resulting log-power images were characterized by a ring of high-power peaks, surrounding a strong, central zero-frequency peak. The zero-frequency offset peak in the power images were masked out for all subsequent processing steps leaving only the ring of high-power peaks. The resulting image

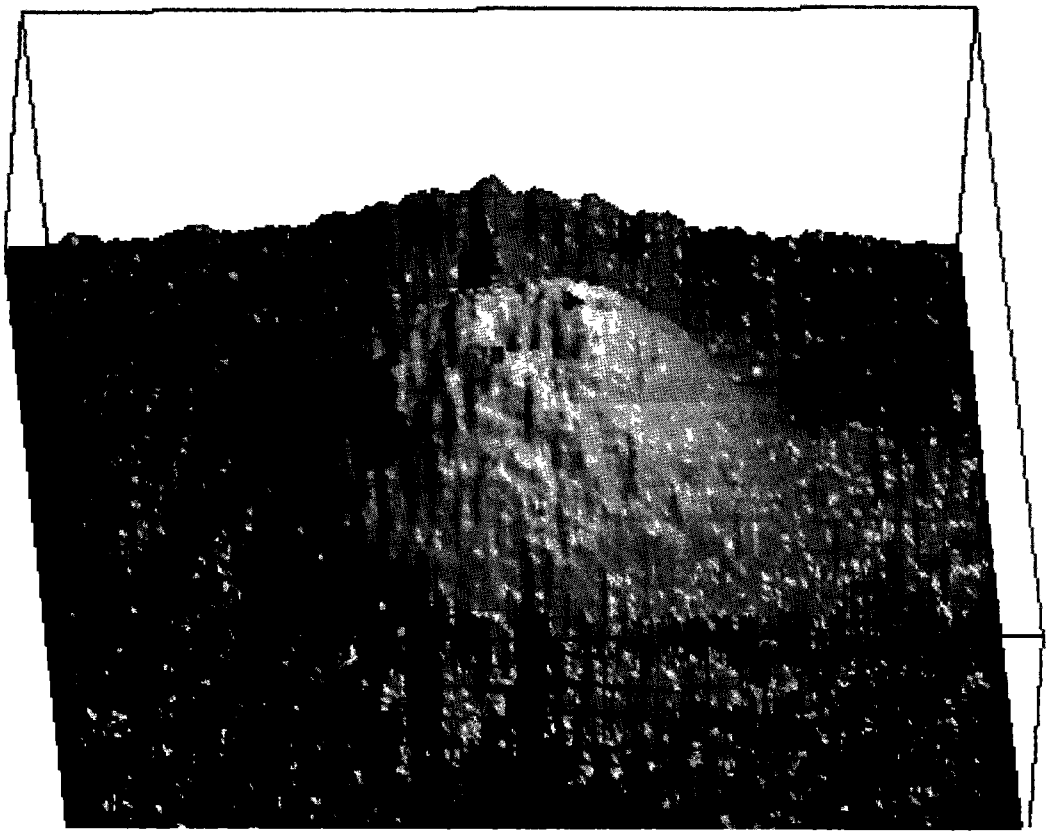

Figure 4. A smoothed (7 × 7) FT power image of the M-Nort site with power on the z axis. The ring of high power surrounding the center of the Fourier transform image was used to derive information of wavelength versus compass direction.

was then smoothed by a 7 by 7 pixel moving average kernel filter. This step enhanced discrimination of the ring of high-power peaks and allowed identification of areas within it with relatively high power (Figure 4).

To highlight the angles at which the greatest degree of periodicity exists, the most powerful point in the high-power ring was found for compass angles ranging from 0° to 180° at 2° intervals. For each angle, the maximum power was recorded. The maximum power for all angles was then rescaled to the range of the expectation length from field mapping and was plotted versus compass angle. This approach does not allow for quantitative analysis of intershrub distances but does allow identification of compass directions most likely to be aligned with streets.

2.3.3. Geostatistical analysis. Unidirectional semivariograms were calculated for each image (Figure 3) for compass angles between 90° and 270° with 2° intervals at lag distances from 0 to 50 m using the equation

$$\gamma(h) = \frac{1}{2n} \sum_{i,j} (V_{t(i,j)+h} - V_{t(i,j)})^2, \qquad (2)$$

where h is a vector with length equal to lag distance and compass direction between 90° and 270°, $\gamma(h)$ is the semivariance at h, i is the east-west spatial coordinate, j is the north-south spatial coordinate, n is the total number of pixels considered, $V_{t(i,j)+h}$ is the value of pixel at $(i, j) + h$, and $V_{t(i,j)}$ is the value of the pixel at (i, j). Every point less than h from the edge of an image was used to calculate the semivariograms.

To determine the isotropic range of spatial autocorrelation for the entire images, omnidirectional semivariograms were calculated by averaging unidirectional semivariograms over 180°. Since average shrub-shrub distance must be equal to the average distance between soil patches, no attempt was made to separate these two signals using semivariogram analysis. This is a general limitation of semivariance analysis.

3. Results

3.1. Field Mapping Results

The field mapping at each site yielded two principal types of information: vegetation cover and estimates of expected street lengths as a function of compass angle. Vegetation cover at the three sites was 25.4, 21.4, and 15.7% for M-Nort, M-Rabb, and M-Well, respectively. These values for vegetative cover are low but are reasonable for the mesquite coppice dunelands represented by each of these sites. The large amount of bare soil at all sites with vegetative cover concentrated in widely separated plants (Figure 3) suggests a high degree of soil nutrient heterogeneity. Inspection of the orthophotos from each site, however, suggests that the average plant diameter at the M-Well site is significantly less than at the M-Nort and M-Rabb sites. Abiotic transport processes are likely to be more important in the distribution of soil resources than biotic transport processes for sites with larger, widely spaced plants [*Schlesinger et al.*, 1990]. The observed larger mesquite plants and intershrub spacing at the M-Nort and M-Rabb sites relative to the M-Well

site suggests that the concentration of soil resources in islands of fertility would be better developed at M-Nort and M-Rabb. Therefore we also expect that a preferred direction of streets would be better developed at these sites compared to M-Well.

Graphs of expected street length versus wind direction support this supposition, with M-Nort and M-Rabb displaying several dominant directions of elongation of bare soil areas between shrubs. M-Well, on the other hand, shows shorter average street lengths with a poorly developed radial pattern (Figure 5). One index of the degree of development of streets at each site is "elongation," the ratio of the maximum expected street length to the minimum expected street length (Table 1). Several points are clear. First, streets at M-Nort are better developed than at any other site. Second, streets at M-Rabb are less well developed than those at M-Nort, and there are two directions of elongation observed at this site. Third, streets at M-Well are the least well developed and show weak east-west orientation.

Helm and Breed [1999] have reported that the majority of erosive winds blow principally toward the east-northeast or west-southwest at a site within 10 km of and on the same kind of topography as M-Nort, M-Rabb, and M-Well (Figure 6). Erosive winds are defined as winds with speeds greater than the wind erosion threshold. Field-mapping results (Figure 5) from M-Nort indicate that streets are oriented with the dominant wind direction. At M-Rabb, one of the street directions is aligned with dominant direction of erosive winds, although this street orientation is less well developed than at M-Nort. At M-Rabb there is also a street direction aligned nearly perpendicular to the street direction at M-Nort.

3.2. Fourier Transform Analysis

FT analysis, wherein peak power is plotted as a function of each compass angle, showed the same directions of elongation as were identified by the field-mapping results (Figure 7, Table 1). Unfortunately, this approach cannot yield quantitative information about the degree of elongation in these directions.

The success for our FT analysis in identifying preferred directions of elongation implies that the directions along which streets are preferentially oriented have a stronger periodicity than other directions. Nonrandom processes must be acting in these directions to enforce the observed periodicity. Wind is the most obvious process that may explain this phenomenon. We hypothesize that streets have a characteristic length and are superimposed on a landscape with more or less random shrub placement.

3.3. Geostatistical Analysis

Unidirectional semivariograms calculated using (2) do not exhibit typical behavior with a well-defined range and a flat sill. Rather, the regular dispersion of the mesquite shrubs gives the sills a weak sinusoidal pattern after a very sharp rise to a local maximum (Figure 8) (see similar analyses in the works of *Phinn et al.* [1996] and *Schlesinger et al.* [1996]). There is currently no theory for the estimation of the statistical significance of sinusoidal sills. The sinusoidal sill is not present in omnidirectional semivariograms, indicating that the periodicity of shrub placement averages out over all directions and beyond some distance shrubs are randomly distributed. However, as unidirectional semivariograms, omnidirectional semivariograms do exhibit a sharp rise to a global maximum (Figure 9).

The maxima in both omnidirectional and unidirectional semivariograms is due to the fact that soil and vegetation form discrete patches in the landscape. Since soil and shrubs display quite different DNs in the images, for distances equal to the average distance between the center of a shrub and the center of the soil patches around it, semivariance will be relatively high. As a result, the location of the maxima in both omnidi-

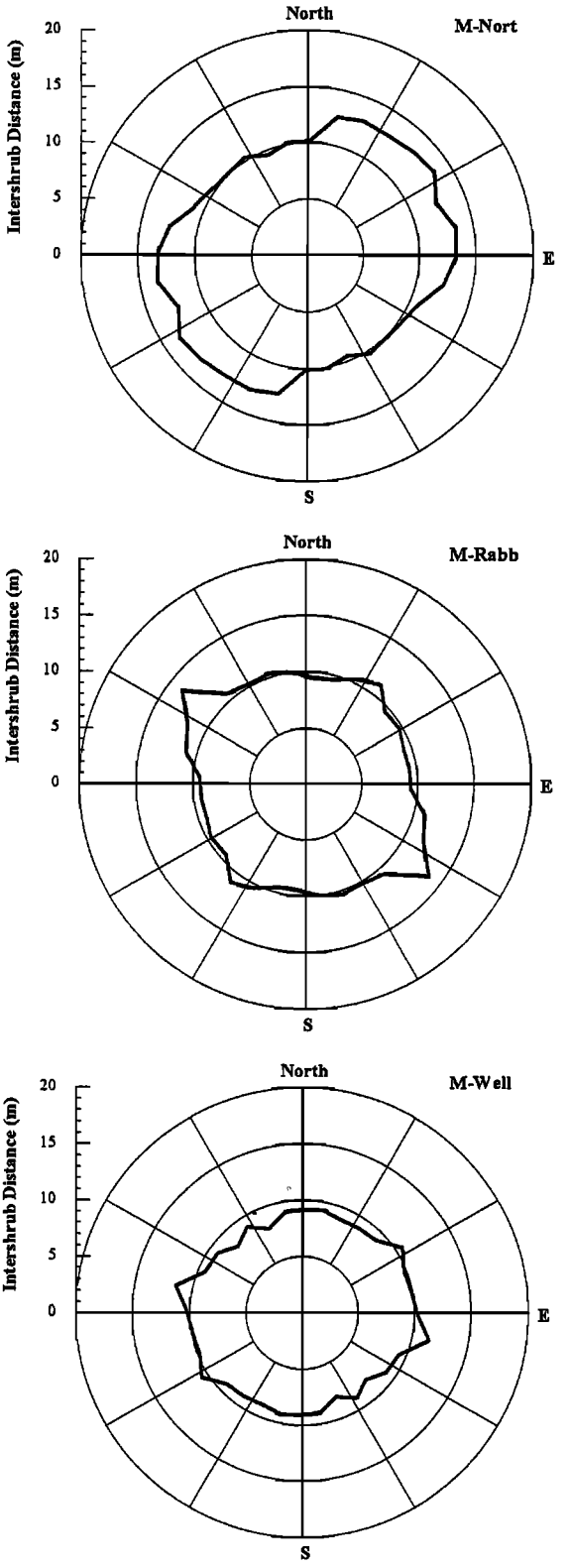

Figure 5. Expected street lengths versus compass direction from field mapping of M-Nort, M-Rabb, and M-Well.

Table 1. Degree of Development of Streets and Direction of Street Elongation Using Various Methods[a]

	M-Nort	M-Rabb	M-Rabb	M-Well
		Field Mapping		
Average width of soil patch, m	11.7	10.3	10.3	9.38
Direction of elongation	45°	295°	25°	90°
Elongation	1.33	1.48	1.18	1.25
		Semivariogram Analysis		
Average shrub-shrub distance, m	15.5	13.2	13.2	10
Direction of elongation	78°	294°–44°	294°–44°	n/a
Elongation	1.42	1.17	1.17	1.00
		FT Analysis		
Direction of elongation	40°	310°	27°	99°

[a]Elongation is the ratio of maximum length to minimum length for field mapping and semivariogram techniques.

rectional and unidirectional semivariograms is interpreted as one-half the average distance between the center of each shrub and the center of its closest neighbors (in a certain direction, for unidirectional semivariograms). Multiplying the lag distance at which this maximum occurs by 2 therefore yields average distance between the center of each shrub in the images and the center of its neighbors. Plots of the average shrub-shrub distance versus compass angle give an indication of the development of streets at each of the sites and display a reasonable correlation with field results (Figure 10).

The shrub-shrub distances derived from omnidirectional semivariograms are larger than the distances between shrubs obtained from the field results (Table 1). This is simply because the field results and semivariogram results are measuring slightly different things: shrub-shrub distances from the semivariograms include the average width of the shrubs, while expected street lengths from field mapping do not. The difference between these two therefore will yield average shrub width, assuming that shrubs themselves are roughly circular. M-Nort displays the largest average shrub width (3.8 m), M-Rabb has an intermediate average shrub width (2.3 m), and M-Well displays the smallest average shrub width (0.62 m).

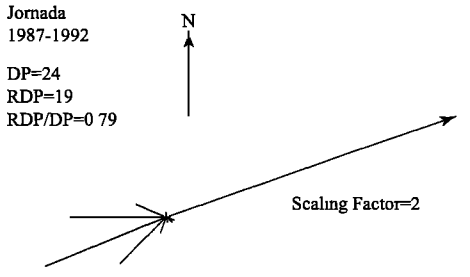

Figure 6. Sand rose for Jornada site. The sandrose is a circular histogram showing mean magnitude and upwind direction of the wind field. The length of the arms are proportional to the potential amount of sand drift from the upwind direction. The length of the resultant arm (arrow) is proportional to the potential net amount of sand moved toward the downwind direction. The lengths of the arms are derived using a weighting equation that applies only to wind speeds above threshold wind speed. The scaling factor is a linear reduction value used to scale the sand rose to the plotting area. DP, drift potential (sand-moving capability of the wind from all directions); RDP, resultant drift potential (net sand-moving capability toward the resultant direction); RDP/DP, an index of directional variability of the wind field (1.00 = no variability). Figure from *Helm and Breed* [1999].

The small shrub diameter at M-Well is consistent with its low relative cover but closer plant spacing. This result is consistent with visual inspection of the DOQ subimages at each site (Figure 3) and supports the idea that islands of fertility are better developed at M-Nort and M-Rabb than at M-Well.

Analysis of the preferred direction of elongation of shrub-shrub distances and elongation in that direction (Table 1) shows that results from the semivariogram analysis are consistent with both the field mapping results and the FT analysis results. Semivariogram analysis was not able to identify two discreet street orientations at M-Rabb, identifying instead a broad region of elongation between the two directions identified by the field-mapping results. In addition, semivariogram analysis was not able to identify a preferred direction of elongation at M-Well. Nonetheless, semivariogram analysis of DOQ images at each of the sites confirmed our assessment of the degree of development of streets at each of the sites. Street development is most prominent at M-Nort, which has the highest elongation ratio, it is intermediate at M-Rabb, and streets are poorly developed at M-Well, which has the lowest elongation ratio (~1).

4. Discussion

4.1. Length and Spacing of Streets

Field mapping as well as FT and geostatistical analysis of DOQs from two of our three mesquite duneland sites suggest the existence of streets. At the third site, M-Well, islands of fertility are poorly developed and there does not appear to be any preferred direction of elongation. Relative to field mapping, the elongations from FT and semivariogram analysis give a poor indication of the characteristics of streets.

There are at least two different distributions of mesquite which might explain elongation of intershrub spaces at preferred directions. In the first distribution (Case 1), every soil patch is slightly elongated and has approximately the same size (Figure 11). Alternatively, consider a landscape in which soil patches are typically not elongate, and all have the same size. In this second type of mesquite distribution, several consecutive shrubs in one direction are "missing," forming a street, with the effect that the average soil patch is elongate (Case 2). In this case, for a regular array of plants, it can be shown that

$$\text{Average Elongation} = \frac{1}{1 - ac(n-1)}, \qquad (3)$$

where a is average intershrub spacing without streets, c is the concentration of streets expressed as streets per meter in the

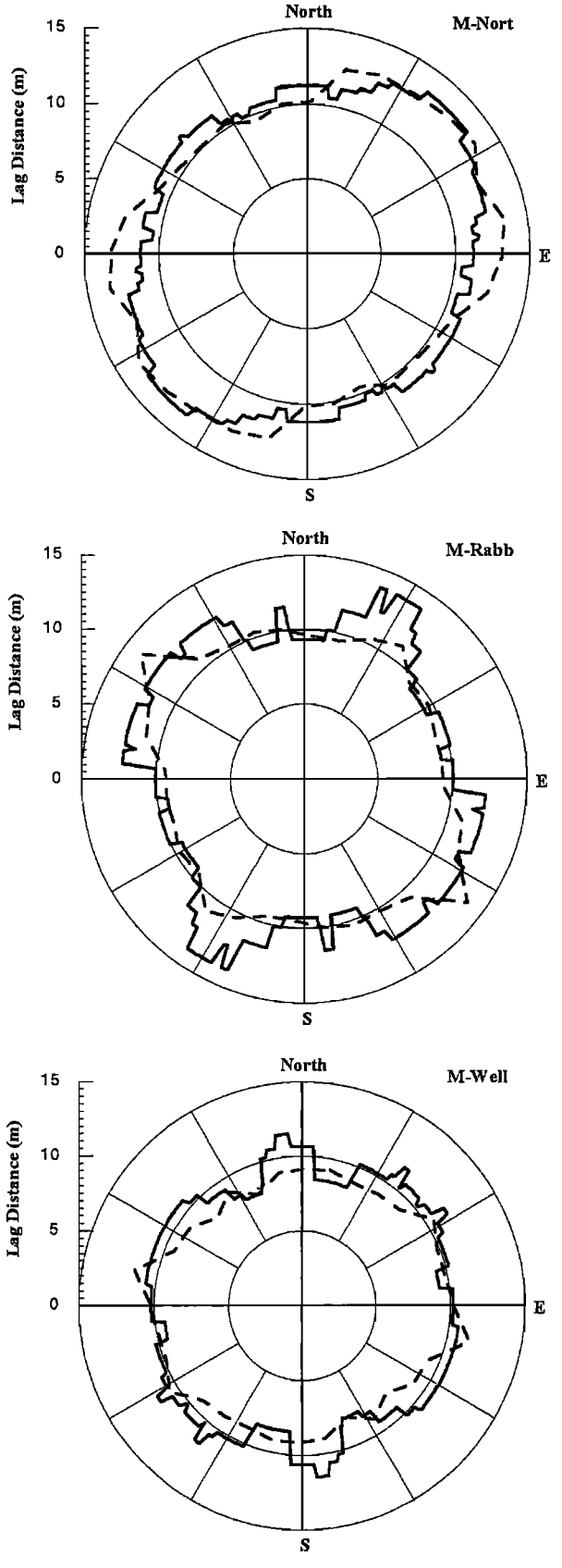

Figure 7. Maximum power versus compass direction from Fourier transform analysis of images of M-Nort, M-Rabb, and M-Well, rescaled to the range of expected street length for each site. Dashed line is expected street length versus compass direction from field mapping.

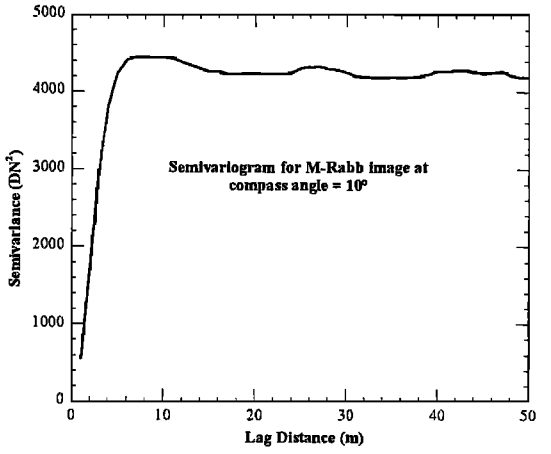

Figure 8. A sample unidirectional semivariogram from the M-Rabb site at 10° compass angle. Note the global maximum near a lag distance of 8 m and the sinusoidal "sill."

street-ward direction, and n is an integer that expresses the length of the streets measured in units of a. A measure of street density with units of streets per plant is defined as $C = ac$, which must be between 0 and 1. Equation (3) is subject to the constraint that $C < (n - 1)^{-1}$ to avoid having a negative number of plants.

Equation (3) allows correlation of the elongation in a particular direction with the expected concentration of streets along that direction. For example, if streets are 3 times as long as the average intershrub spacing of 10 m ($n = 3$, $a = 10$ m), then for an average elongation of 1.5, the concentration of streets must be 0.0167 m^{-1}. In other words, streets are separated from each other in the street-ward direction by 60 m in this case.

Previous field and laboratory experiments allow evaluation of the two possible cases for distributions of mesquite at Jornada (Cases 1 and 2). Wind tunnel experiments by *Minvielle et al.* [1999] simulated mesquite bushes arranged so that streets were present. Measured turbulent intensities show the existence of a wake for distances approaching an order of magni-

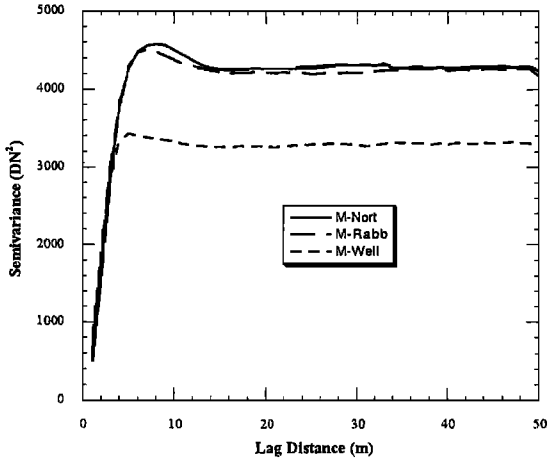

Figure 9. Omnidirectional semivariogram calculated from images of M-Nort, M-Rabb, and W-Well. Note that the sill is flat compared to unidirectional semivariograms (Figure 8). The location of the maximum for each semivariogram is equal to one-half the average intershrub spacing at each site.

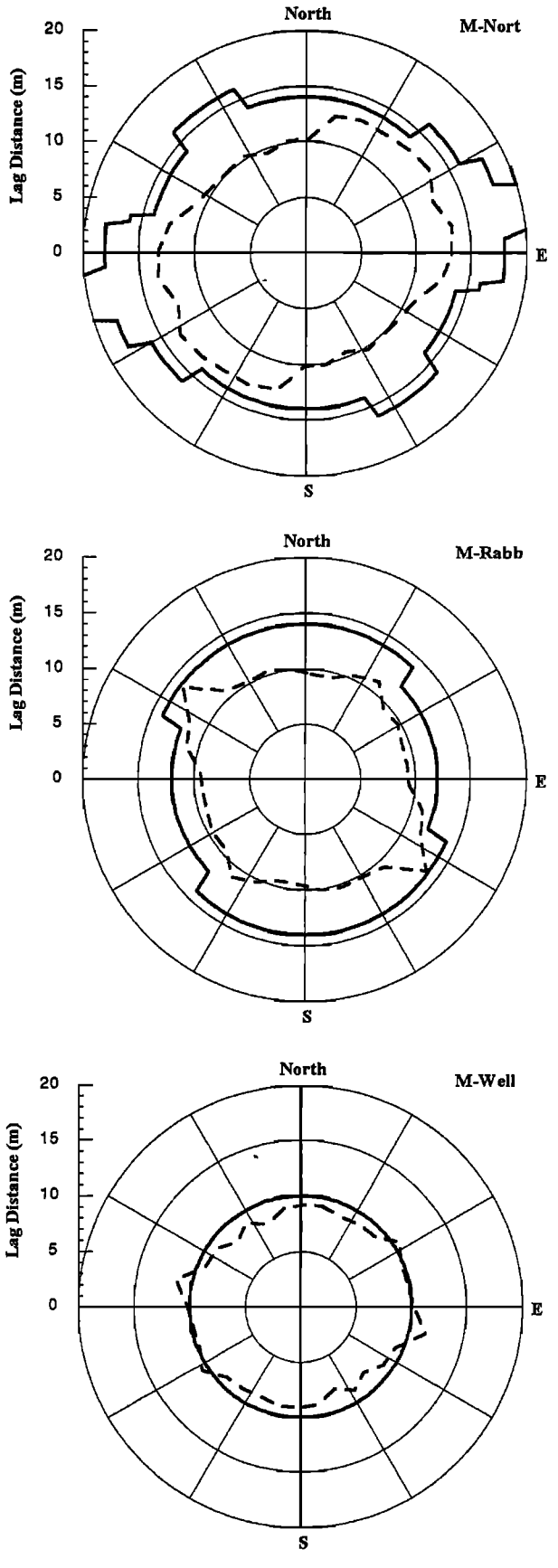

Figure 10. Shrub-shrub distance versus compass direction from unidirectional semivariogram analysis of images of M-Nort, M-Rabb, and M-Well. Dashed line is expected street length versus compass direction from field mapping.

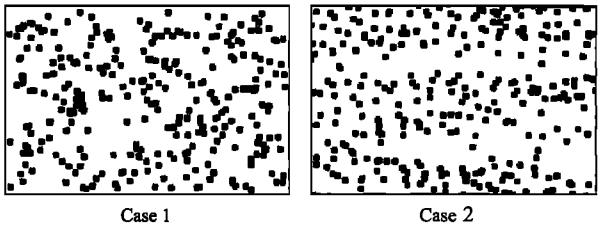

Figure 11. Two possibilities to explain the observed elongation of intershrub distances from field, FT, and geostatistical analyses. Case 1: shrubs are uniformly distributed with average intershrub distance greater in horizontal direction. Case 2: streets exist as a few long areas of bare soil interspersed in areas where mesquite have intershrub distances near the average.

tude greater than the height of the simulated mesquite bushes. Thus downwind of the simulated mesquite bushes, there is a zone of protection that lowers winds for distances of up to an order of magnitude greater than the height of the bush. In the streets, there is no zone of protection.

Gillette and Monger [2000] have shown that desert areas dominated by mesquite having the same biomass as other shrubland areas produce more dust by ratios ranging from 4 : 1 to 8 : 1. *Minvielle et al.*'s [1999] laboratory simulations show that this observed increase in dust production could not result from Case 1, where street-ward shrub spacing has to be at least 10 times the average shrub height. For reasonable elongations (1.5) and mesquite dune heights (2 m), average shrub spacing would have to be ~20 m. This average distance between shrubs is greater than that from field and geostatistical analysis of mesquite sites at Jornada. Furthermore, in a field experiment, *Gillette and Chen* [2000] have reported that sand fluxes show a monotonic increase as the upwind distance from the shelter of vegetation increases. This supports Case 2, where dust production is enhanced by a few large-fetch areas. Finally, field results indicate that very long streets (>32 m) are much more probable in street-ward directions compared to cross-street directions (Figure 12). We conclude that streets exist in mesquite dunelands as a few long (relative to average shrub spacing) areas of bare soil interspersed in areas where mesquite have more average distances between shrubs.

4.2. Implications for Land-Atmosphere Interactions and Wind Erosion Modeling

Dust emission from the world's deserts is a major source of global atmospheric aerosols which have been implicated in increasing planetary albedo, thus serving as a potential check on anthropogenic global warming [*Andreae*, 1996]. The existence of streets and the associated elevated dust fluxes indicate that dust fluxes from shrublands around the globe may be much higher than previously thought. In addition, the development of streets in landscapes that underwent recent grassland-shrubland conversion suggests that during the transition, the landscape self-organizes to maximize wind erosion. Therefore land use and land cover change need to be incorporated into large-scale atmospheric models in order to make accurate estimates of dust flux and aerosol concentrations.

Semivariogram and FT analysis of 1-m DOQs may be used to identify areas where streets exist and to determine the principal street orientations. Thus they may also provide important information for detailed wind erosion modeling in arid and

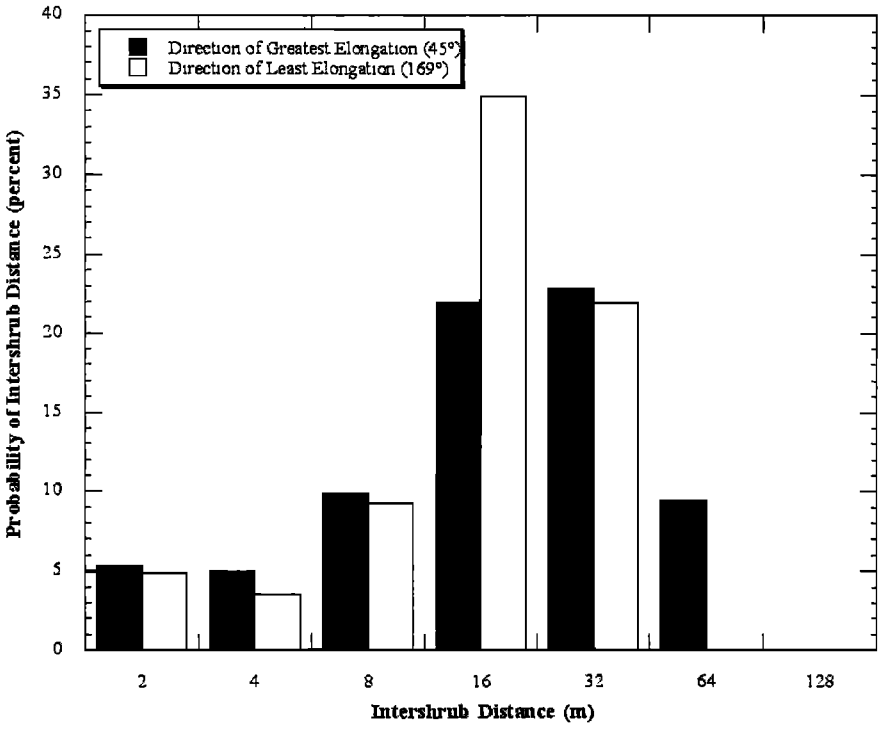

Figure 12. Probability of areas of continuous bare soil with length given on the x axis at the M-Nort site for the direction of greatest and least elongation.

semiarid regions. Areas with streets are likely to exhibit increased wind erosion relative to areas without streets with the same vegetation biomass. All current mathematical models of wind erosion that take vegetation into account assume homogenous distribution of plants [e.g., *Wolfe and Nickling*, 1993]. Areas with streets are markedly anisotropic and exhibit increased wind erosion and dust production. New methods to estimate wind erosion must be developed which take this anisotropy into account.

4.3. Implications for Landscape Processes

Desertification has been defined as the loss or spatial redistribution of net primary productivity in arid and semiarid lands [*Schlesinger et al.*, 1990]. The islands of fertility, centered around large perennial shrubs, which result from desertification processes are enforced by abiotic transport in degraded lands. Recent work by *Schlesinger et al.* [1999] has shown that increased water erosion can lead to increased losses of plant-available N and enforcement of islands of fertility in degraded semiarid landscapes. *Klausmeir* [1999] has shown that water erosion can produce inhomogenous vegetation distributions, and therefore islands of fertility, even in very low relief landscapes. Our work on streets in mesquite dunelands indicates that wind also plays a role in the enforcement of islands of fertility. Wind therefore may be an important factor in landscape evolution as homogenous distributions of soil resources in grasslands are supplanted by heterogeneous distributions in shrublands.

In particular, the alignment of streets at both the M-Nort and the M-Rabb sites with the prevailing direction of erosive winds indicates that wind itself played a vital role in the evolution of this landscape as it made the transition from grassland to shrubland in the last 150 years [*Buffington and Herbel*, 1965]. We hypothesize that as the landscape became increasingly infested with woody shrubs, areas between shrubs became the sites of wind erosion. As the most erosive winds typically blow from one principal direction at Jornada (Figure 6), areas of bare soil that were aligned with the prevailing wind (protostreets) saw a number of effects that more protected areas did not. These effects include (1) increased saltation of sand grains and sandblasting of plants in the protostreets leading to increased mortality of plants in these areas, particularly seedlings and grasses with little effect on the wind profile, (2) increased winnowing of fine particles in the protostreets leading to decreased water-holding capacity and nutrient availability in these areas [*Okin et al.*, 2001b], and (3) depletion of the seed bank in protostreets as light, wind-movable seeds were progressively blown out of these areas. The combined effect of the increased wind activity in the protostreets suppressed vegetation in these areas, leading to the establishment of mature streets which remain areas of increased wind erosion and dust production. The effect of wind in the development of landscape structure would be greatest in areas with fine-grained soils susceptible to wind erosion. Grassland to shrubland transitions in landscapes with wind-stable soils are not so likely to develop streets, because winnowing of fines and sandblasting would be smaller [*Okin et al.*, 2001b].

Mature streets, even if they are not aligned with the prevailing wind direction such as one of the street directions at M-Rabb, are self-enforcing phenomena. When the wind does blow in the direction of a street, it is the site of increased wind erosion, even if it is not oriented with the prevailing wind. A few storms a year with winds aligned with a street, combined with other elements of intershrub competition for soil resources, may be all that is needed to prevent new plants from growing in established streets. Thus once a fabric of streets is established, it is likely to be a permanent feature in the landscape.

Even in landscapes with wind-erodible soils, street development may not be ensured. At the M-Well site, little street development is seen though this site underwent grassland to shrubland conversion at approximately the same time as the other sites [*Buffington and Herbel*, 1965]. This may be due to the fact that this site is underlain by a thick, impermeable caliche layer which may have been exposed by wind erosion near the time of mesquite establishment. The resulting shallow rooting zone therefore is less amenable to deep-rooted mesquite and inhibits their growth. Mesquites at this site therefore may have smaller overall horizontal root structures allowing them to be closer together. This may explain the larger number of smaller mesquite at this site and also the lack of well-developed streets. In order for streets to develop, bare areas at least 10 times the average shrub height are required [*Minvielle et al.*, 1999]. At M-Well, however, mesquite are closely spaced and thus streets are not well developed.

Schlesinger et al. [1990] suggested that the development of shrub-centered islands of fertility associated with the degradation of semiarid grasslands was accompanied by a net loss of nutrients as the transition from grassland to shrubland occurred. This has been verified by *Schlesinger et al.* [1996] in a subsequent paper with detailed soil analyses in a variety of arid shrubland and semiarid grassland environments. In ongoing work on the role of surface runoff, *Schlesinger et al.* [2000] have concluded that loss of soil nutrients by hillslope runoff cannot, by itself, account for the depletion of soil fertility associated with desertification in the Chihuahuan Desert.

Alternatively, wind erosion may prove to be a mechanism to explain widespread nutrient loss in degraded arid and semiarid environments. We hypothesize that the elevated dust emission observed in mesquite shrublands may contribute to the observed and postulated loss of nutrients from these landscapes [*Schlesinger et al.*, 1990, 1996]. N and P are concentrated on wind-erodible particles which are removed permanently by wind erosion [*Leys and McTainsh*, 1994; *Larney et al.*, 1998]. Soil N and P concentrations at a nearby site in the Jornada basin have been measured by *Okin et al.* [2001a]. Their results indicate an 80% net loss of available N and a 70% net loss of plant-available P from a site free of vegetation during 8 years, suggesting that wind erosion impacts soil fertility in actively deflating areas. Further work should be pursued to address the role of wind in removing nutrients from degraded landscapes as well as the role of wind in enforcing islands of fertility in shrublands.

5. Conclusions

The existence of streets in areas of mesquite shrubs is a potentially important factor enhancing dust production. The purpose of this study was to (1) confirm the existence of streets in mesquite dunelands, (2) develop image-processing techniques that are able to identify the presence and orientation of streets and can be used generally to identify landscapes with streets, and (3) address the implications of the existence of streets for the evolution of arid and semiarid environments.

Through the use of field mapping as well as FT and semivariogram analysis we show that mesquite dunelands in the Chihuahuan Desert of southern New Mexico, United States, have inhomogenous shrub distributions. Streets exist in these landscapes but may be better developed in some areas compared to others. Soils in the streets are not protected from winds blowing down the streets and may therefore produce more dust than if vegetation were more evenly distributed. This may partially explain discrepancies between observed and predicted atmospheric dust concentrations. New models to incorporate the existence of streets are required if models of dust flux are to be realistic for these landscapes. Without such models, reliable estimates of the effect of land use and land cover change in the world's drylands on atmospheric aerosol concentrations will be extremely difficult. Furthermore, the existence of streets implies that wind plays a major role in the evolution of vegetated arid and semiarid landscapes with wind-erodible soils. It enforces islands of fertility centered around individual shrubs, prohibits vegetation growth between shrubs, and may provide an explanation for reduced soil fertility observed in shrublands. Further work is required to clarify the role of wind erosion in the degradation of semiarid landscapes undergoing grassland to shrubland conversion as well as the effect of this conversion on atmospheric aerosol concentrations.

Acknowledgments. Lawrence (Sam) Bothern and Michael Townsend carefully carried out the field measurements for the maps. W. Schlesinger provided valuable advice and guidance during the experimentation. This research was carried out as part of the Long-Term Ecological Research program at the Jornada del Muerto site. During this study, the program was administered by Duke University and supported by the National Science Foundation grant DEB 94-11971.

References

Andreae, M. O., Raising dust in the greenhouse, *Nature*, *380*, 389–390, 1996.

Ayoub, A., Extent, severity and causative factors of land degradation in the Sudan, *J. Arid Environ.*, *38*(3), 397–409, 1998.

Bach, A. J., Assessing conditions leading to severe wind erosion in the Antelope Valley, California, 1990–1991, *Prof. Geogr.*, *50*(1), 87–97, 1998.

Barth, H., Desertification in the Eastern Province of Saudi Arabia, *J. Arid Environ.*, *43*(4), 399–410, 1999.

Buffington, L. C., and C. H. Herbel, Vegetational changes on a semidesert grassland range from 1858 to 1963, *Ecol. Monogr.*, *35*(2), 139–164, 1965.

Bulloch, H. E., Jr., and R. E. Neher, *Soil Survey of Dona Ana County Area, New Mexico*, Soil Conserv. Serv., U.S. Dep. of Agric., Washington, D. C., 1977.

Çevik, B., and A. Berkman, Wind erosion control and sand dune stabilization practices implemented in the Great Konya Basin of Turkey, in *International Workshop on Sand Transport and Desertification in Arid Lands*, edited by F. El-Baz, I. A. El-Tayeb, and M. H. A. Hassan, pp. 375–388, World Sci., Khartoum, Sudan, 1985.

Darkoh, M. B. K., Combating desertification in the arid and semi-arid lands of Tanzania, *J. Arid Environ.*, *12*(2), 87–99, 1987.

El-Baz, F., I. A. El-Tayeb, and M. H. A. Hassan, Sand transport and desertification in arid lands, in *International Workshop on Sand Transport and Desertification in Arid Lands*, edited by F. El-Baz, I. A. El-Tayeb, and M. H. A. Hassan, 472 pp., World Sci., Khartoum, Sudan, 1985.

Gillette, D. A., and W. Chen, Particle production and aeolian transport from a "supply-limited" source area in the Chihuahuan Desert, *J. Geogr. Res.*, in press, 2000.

Gillette, D. A., and R. Passi, Modeling of dust emission caused by wind erosion, *J. Geophys. Res.*, *93*, 14,223–14,242, 1988.

Helm, P., and C. S. Breed, Instrumented field studies of sediment transport by wind, in *Desert Winds: Monitoring Wind-Related Surface Processes in Arizona, New Mexico, and California*, edited by C. S. Breed and M. Reheis, *USGS Prof. Pap. 1598*, pp. 30–51, U.S. Govt. Print. Off., Washington, D. C., 1999.

Khalaf, F. I., Desertification and aeolian processes in the Kuwait Desert, *J. Arid Environ.*, *16*(2), 125–145, 1989.

Kishk, M. A., Desert encroachment on the fringes of the Nile Valley, Egypt, in *International Workshop on Sand Transport and Desertifica-*

tion in Arid Lands, edited by F. El-Baz, I. A. El-Tayeb, and M. H. A. Hassan, pp. 196–208, World Sci., Khartoum, Sudan, 1985.

Klausmeier, C. A., Regular and irregular patterns in semiarid vegetation, *Science*, *284*, 1826–1828, 1999.

Larney, F., M. Bullock, H. Janzen, B. Ellert, and E. Olson, Wind erosion effects on nutrient redistribution and soil productivity, *J. Soil Water Conserv.*, *53*(2), 133–140, 1998.

Leys, J., and G. McTainsh, Soil loss and nutrient decline by wind erosion- cause for concern, *Aust. J. Soil Water Conserv.*, *7*(3), 30–35, 1994.

Leys, J. F., and G. H. McTainsh, Sediment fluxes and particle grain-size characteristics of wind-eroded sediments in southeastern Australia, *Earth Surface Processes and Landforms*, *21*, 661–671, 1996.

Luk, S.-H., Recent trends in desertification in the Maowusu Desert, China, *Environ. Conserv.*, *10*, 213–224, 1983.

Marticorena, B., and G. Bergametti, Modeling the atmospheric dust cycle, 1, Design of a soil-derived dust emission scheme, *J. Geophys. Res.*, *100*, 16,415–16,430, 1995.

Marticorena, B., G. Bergametti, B. Aumont, Y. Callot, C. N'Doumé, and M. Legrand, Modeling the atmospheric dust cycle, 2, Simulation of Saharan sources, *J. Geophys. Res.*, *102*, 4387–4404, 1997.

Minvielle, F. B., B. Marticorena, D. A. Gillette, R. Lawson, and R. Thompson, *Study of Roughness Length for Low Roughness Densities and Several Porosities*, Fluid Model. Facil., U.S. Environ. Prot. Agency, Research Triangle Park, N. C., 1999.

Musick, H. B., and D. A. Gillette, Field evaluation of relationships between a vegetation structural parameter and sheltering against wind erosion, *Land Degrad. Rehab.*, *2*, 87–94, 1990.

Okin, G. S., B. Murray, and W. H. Schlesinger, Desertification in an arid shrubland in the southwestern United States: Process modeling and validation, in *Land Degradation*, edited by A. Conacher, Kluwer Acad., Norwell, Mass., in press, 2001a.

Okin, G. S., W. H. Schlesinger, and B. Murray, Degradation of paleolake shrubland environments, *J. Arid Environ.*, *47*, 124–144, 2001b.

Paulsen, H. A., Jr., and F. N. Ares, Grazing values and management of black gramma and tobosa grasslands and associated shrub ranges of the Southwest, U.S. Forest Serv., Washington, D. C., 1962.

Phinn, S., J. Franklin, A. Hope, D. Stow, and L. Huenneke, Biomass distribution mapping using airborne digital video imagery and spatial statistics in a semiarid environment, *J. Environ. Manage.*, *47*, 139–164, 1996.

Schlesinger, W. H., J. F. Reynolds, G. L. Cunningham, L. F. Huenneke, W. M. Jarrell, R. A. Virginia, and W. G. Whitford, Biological feedbacks in global desertification, *Science*, *247*, 1043–1048, 1990.

Schlesinger, W. H., J. A. Raikes, A. E. Hartley, and A. F. Cross, On the spatial pattern of soil nutrients in desert ecosystems, *Ecology*, *77*(2), 364–374, 1996.

Schlesinger, W. H., A. D. Abrahams, A. J. Parsons, and J. Wainwright, Nutrient losses in runoff from grassland and shrubland habitats in Southern New Mexico, I, rainfall simulation experiments, *Biogeochemistry*, *45*, 21–34, 1999.

Schlesinger, W. H., T. J. Ward, and J. Anderson, Nutrient losses in runoff from grassland and shrubland habitats in southern New Mexico, II, Field plots, *Biogeochemistry*, *49*, 69–86, 2000.

Shao, Y., and L. M. Leslie, Wind erosion prediction over the Australian continent, *J. Geophys. Res.*, *102*, 30,091–30,105, 1997.

Stockton, P. H., and D. A. Gillette, Field measurement of the sheltering effect of vegetation on erodible land surfaces, *Land Degrad. Rehab.*, *2*, 77–85, 1990.

Wilshire, H. G., Human causes of accelerated wind erosion in California's deserts, in *Thresholds in Geomorphology*, edited by D. R. Coates and J. D. Vitek, pp. 415–433, George, Allen and Unwin, London, England, 1980.

Wolfe, S. A., and W. G. Nickling, The protective role of sparse vegetation in wind erosion, *Progr. Phys. Geogr.*, *17*, 50–68, 1993.

Zhao, S., Drifting sand hazard and its control in northwest arid China, in *International Workshop on Sand Transport and Desertification in Arid Lands*, edited by F. El-Baz, I. A. El-Tayeb, and M. H. A. Hassan, pp. 253–266, World Sci., Khartoum, Sudan, 1985.

D. A. Gillette, Atmospheric Sciences Modeling Division, Air Resources Laboratory, National Oceanic and Atmospheric Administration, Research Triangle Park, NC 27711.

G. S. Okin, Department of Geography, University of California, Santa Barbara, CA 93106. (okin@gps.caltech.edu)

(Received June 19, 2000; revised December 15, 2000;
accepted January 8, 2001.)